SUPPORTING INFORMATION

Fabrication of CdS/Pt/MIL-125 with effective spatial separation for improved visible-light catalytic H_2 evolution by using γ-ray irradiation

Chen Tai,[†] Huarong Liu,[*,†] Yuan Hu[‡]

[†]CAS Key Laboratory of Soft Matter Chemistry, Department of Polymer Science and Engineering, University of Science and Technology of China, Jinzhai Road 96, Hefei, Anhui 230026, P. R. China

[‡]State Key Laboratory of Fire Science, University of Science and Technology of China, Jinzhai Road 96, Hefei, Anhui 230026, P. R. China

* Corresponding author:

Email address: hrliu@ustc.edu.cn (H. R. Liu); Tel: +86 551 63601586

The number of pages: **12**

The number of Figures: **14**

The number of Tables: **4**

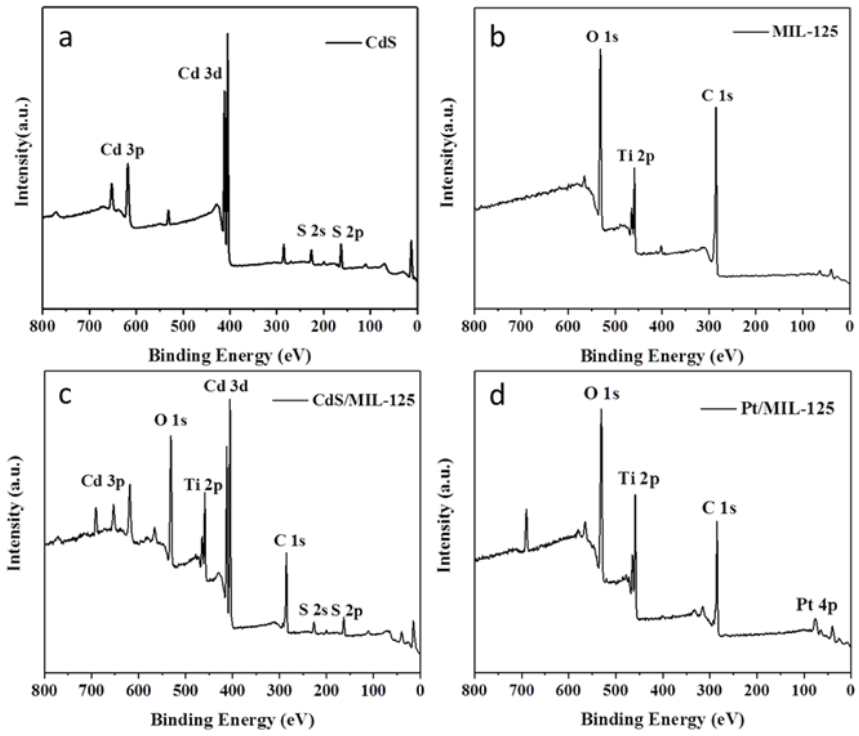

Figure S1. XPS survey scan of (a) CdS, (b) MIL-125, (c) CdS3/MIL-125 and (d) Pt4/MIL-125.

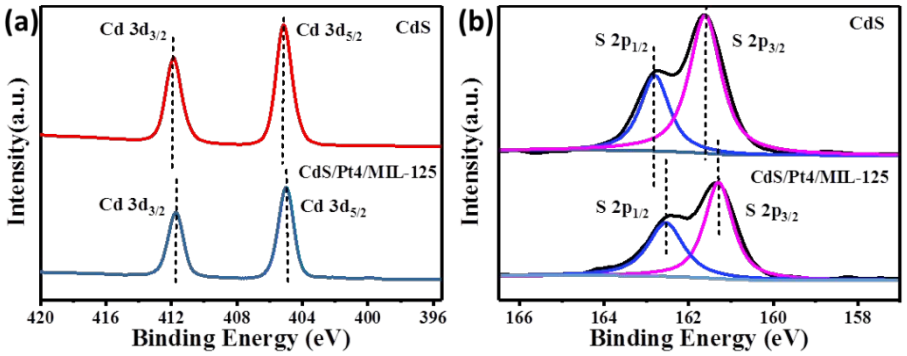

Figure S2. The high-resolution XPS spectra of CdS and CdS/Pt4/MIL-125: (a) Cd 3d and (b) S 2p.

Table S1. Specific surface area, average pore size and pore volume of CdS, MIL-125, Pt4/MIL-125, CdS3/MIL-125, Pt/CdS/MIL-125 and CdS/Pt4/MIL-125.

Catalysts	Surface Area ($m^2\ g^{-1}$)	Average Pore Size (nm)	Pore Volume ($cm^3\ g^{-1}$)
CdS	54.65	7.93	0.065
MIL-125	1214	1.64	0.633
Pt4/MIL-125	885.0	1.70	0.461
CdS3/MIL-125	383.1	4.08	0.283
Pt/CdS/MIL-125	209.3	4.95	0.233
CdS/Pt4/MIL-125	194.9	6.41	0.231

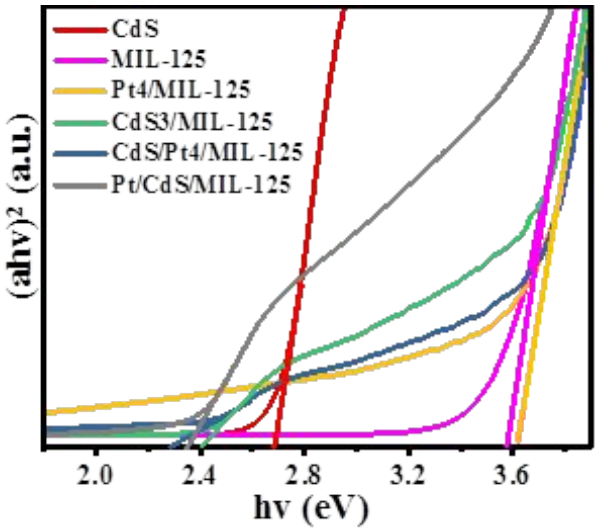

Figure S3. The corresponding plots of transformed Kubelka–Munk functions versus light energy of CdS, MIL-125, Pt4/MIL-125, CdS3/MIL-125, CdS/Pt4/MIL-125 and Pt/CdS/MIL-125.

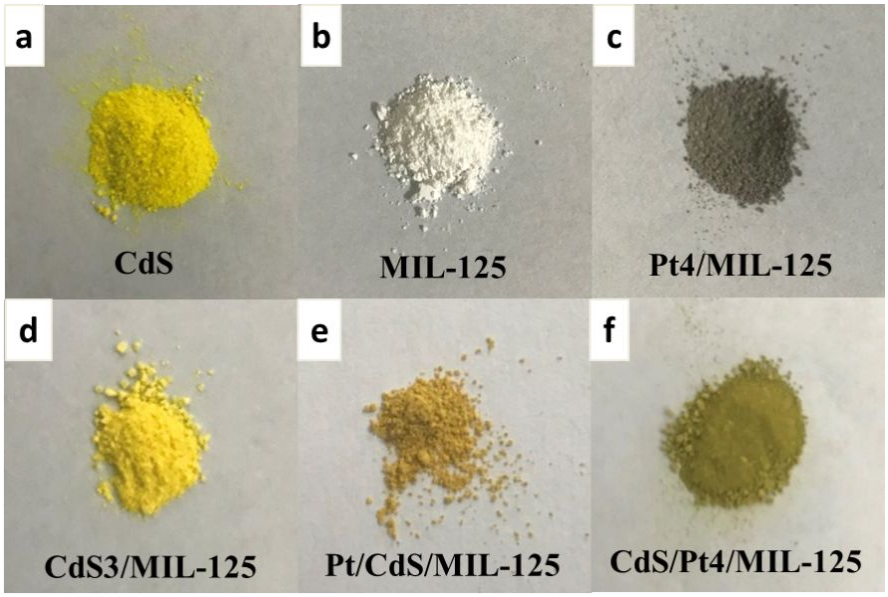

Figure S4. Photos of (a) CdS, (b) MIL-125, (c) Pt4/MIL-125, (d) CdS3/MIL-125, (e) Pt/CdS/MIL-125 and (f) CdS/Pt4/MIL-125.

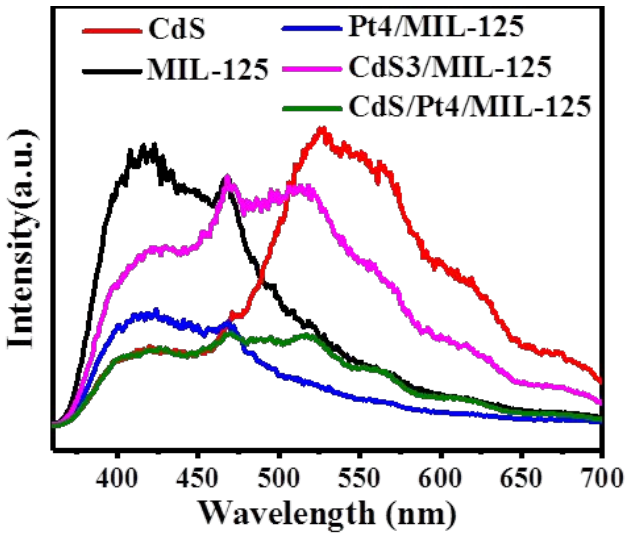

Figure S5. Photoluminescence spectra of MIL-125, CdS, Pt4/MIL-125, CdS3/MIL-125 and CdS/Pt4/MIL-125.

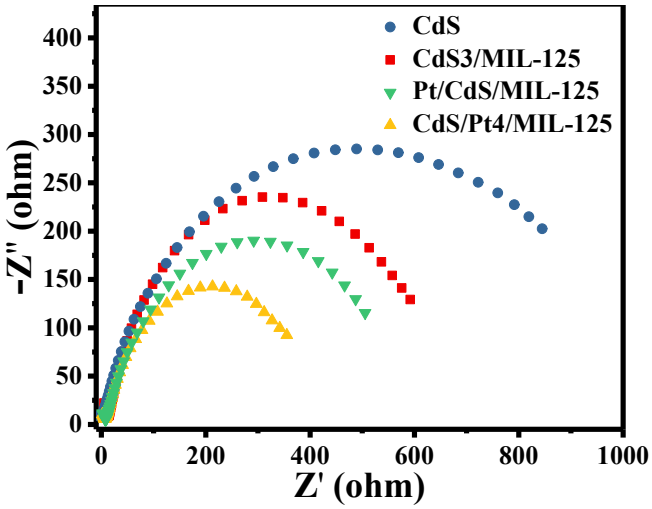

Figure S6. EIS Nyquist plots for CdS, CdS3/MIL-125, Pt/CdS/MIL-125 and CdS/Pt4/MIL-125.

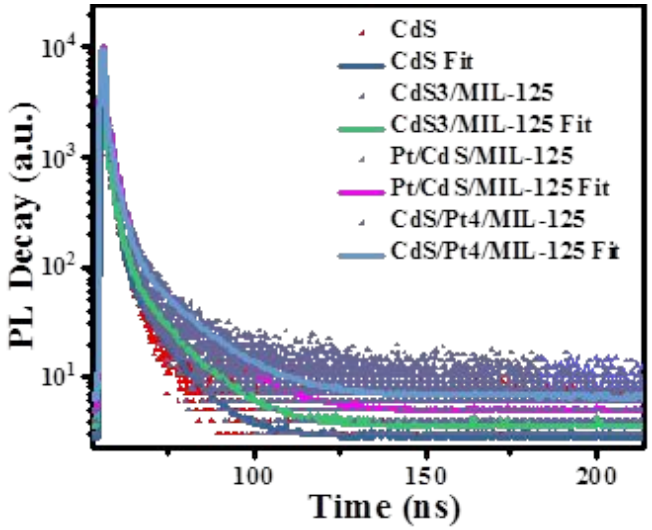

Figure S7. Time-resolved transient fluorescence spectra of CdS, CdS3/MIL-125, Pt/CdS/MIL-125 and CdS/Pt4/MIL-125 excited at 370 nm.

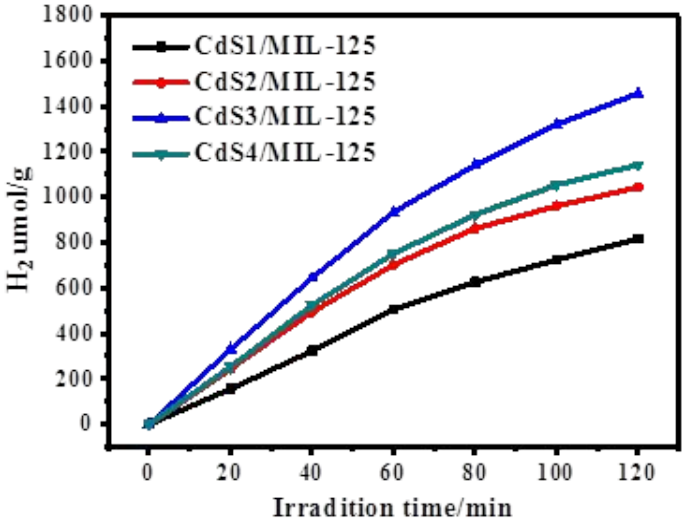

Figure S8. Time courses of H_2 evolution over CdS/MIL-125 catalysts with different amounts of CdS under the conditions: catalysts (20 mg), 0.1 M Na_2S-Na_2SO_3 (40 mL), light source of Xe lamp (300 W) with a cut-off filter ($\lambda \geq 420$ nm).

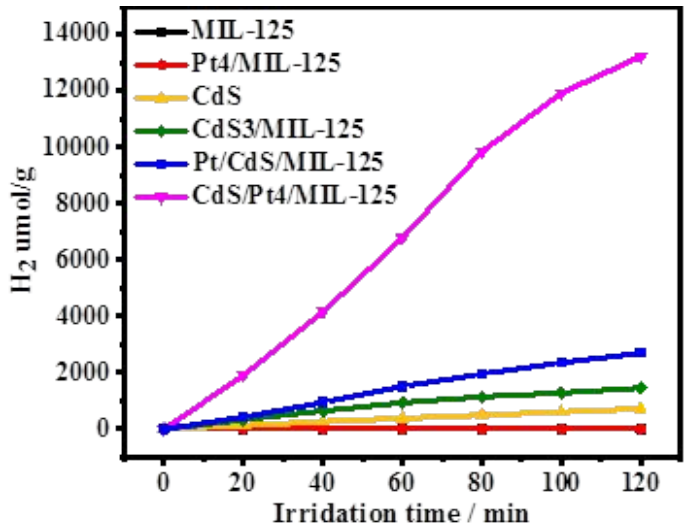

Figure S9. Time courses of H_2 evolution based on the first hour over various catalysts under the conditions: catalysts (20 mg), 0.1 M Na_2S-Na_2SO_3 (40 mL); light source of Xe lamp (300 W) with a cut-off filter ($\lambda \geq 420$ nm).

Table S2. The contents of Pt and Cd of different samples.

Sample	**Cd Metal content** (wt%)		**Pt Metal content** (wt%)	
	Theoreticle value	**ICP-MS result**	**Theoreticle value**	**ICP-MS result**
CdS2/MIL-125	27.6	18.8	-	-
CdS3/MIL-125	32.2	24.1	-	-
CdS/Pt5/MIL-125	31.2	23.3	2.88	1.52
CdS/Pt4/MIL-125	31.4	23.9	2.48	1.10
Pt/CdS/MIL-125	31.4	23.7	2.48	1.15

Table S3. Comparison of CdS/Pt4/MIL-125 nanocomposite with other photocatalysts.

Catalyst	Experimental condition	Hydrogen evolution rate ($\mu mol \cdot g^{-1} \cdot h^{-1}$)	AQE (%)	Ref.
TiO_2-Au-CdS	0.1 g catalyst, 40 mL of water containing Na_2S (0.1 M), Na_2SO_3 (0.1 M), 300 W Xe lamp, $\lambda > 420$ nm	1810	-	S1
CdS-MCM-48-50	0.04 g catalyst, 20 mL of 1:1 ethanol/water, 300 W Xe lamp, $\lambda >$ 400 nm	1150	10.5	S2
CdS@TiO_2@Au	0.02 g catalyst, 40 mL of water containing Na_2S (0.1 M), Na_2SO_3 (0.1 M), 300 W Xe lamp, $\lambda > 400$ nm	1720	12.9	S3
ZnO/CdS/ZnS	0.01 g catalyst, 10 mL of water containing Na_2S (0.35 M), Na_2SO_3 (0.25 M), 300 W Xe lamp, $\lambda > 400$ nm	2077	-	S4
UIO-66/CdS(10)	0.016 g catalyst, 31 mL of 27:3:1 CH_3CN/lactic acid/H_2O, 300 W Xe lamp, $\lambda > 380$ nm	1725	0.64	S5

NH_2-MIL-125/TiO_2/CdS	0.05 g catalyst, 60 mL aqueous solution of $Na_2S·9H_2O$ (0.2 M) , Na_2SO_3 (0.3 M) and 0.3 wt % Pt, 300 W Xe lamp, λ > 400 nm	2997.482	4.81	S6
H-TiO_2/CdS		1970. 813	2.19	
CdS/Pt4/MIL-125	0.02 g catalyst, 40 mL of water containing Na_2S (0.1 M), Na_2SO_3 (0.1 M), 300 W Xe lamp, λ > 400 nm	6783.5	7.3	This work

The calculation of apparent quantum efficiency

The apparent quantum efficiency (AQE) of the CdS/Pt4/MIL-125 sample was measured under the photocatalytic reaction condition (20 mg of catalysts in 40 mL solution of 0.1 M Na_2S and 0.1M Na_2SO_3) using 300 W Xe lamp equipped with the band-pass filters of wavelengths. The AQE was calculated by the following equation:

$$AQE = \frac{number\ of\ reacted\ electrons}{number\ of\ incident\ photons} \times 100\%$$

$$= \frac{number\ of\ evolved\ H_2\ molecules\ \times\ 2}{number\ of\ incident\ photons} \times 100\%$$

$$= \frac{n_{H_2} \times N_A \times 2}{E\lambda/hc} \times 100\% \qquad \textbf{(S1)}$$

Equation S1. The calculation equation of AQE for the photocatalysts.

For instance, the above formula can be used to make the following calculation for the AQE at the wavelength of 420 nm for CdS/Pt4/MIL-125 with the required experimental parameters, including the power density of Xenon lamp at 420 nm (2.04 mW/cm^{-2}), the active area under irradiation light (15.3 cm^2) and the molar of generated hydrogen in 2 h (28.9 μmol).

Table S4. The apparent quantum efficiency (AQE) of CdS, CdS3/MIL-125, Pt/CdS/MIL-125 and CdS/Pt4/MIL-125 for hydrogen evolution.

Sample	AQE (%)
CdS	1.9
CdS3/MIL-125	3.1
Pt/CdS/MIL-125	4.0
CdS/Pt4/MIL-125	7.3

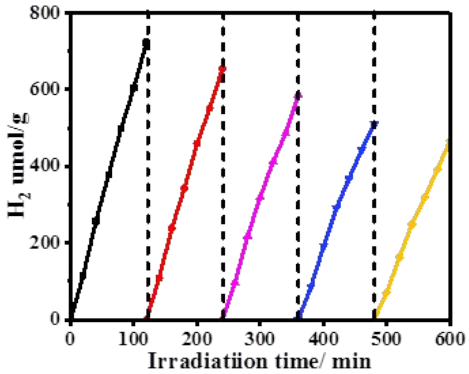

Figure S10. Recycling tests of photocatalytic H_2 evolution of CdS nanopaticles.

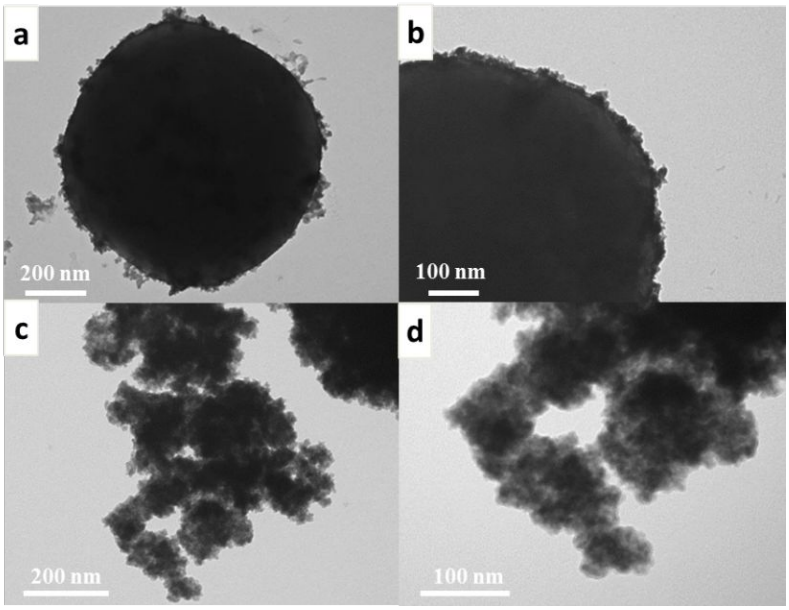

Figure S11. TEM images of (a, b) CdS/Pt4/MIL-125 and (c, d) CdS after cycling tests.

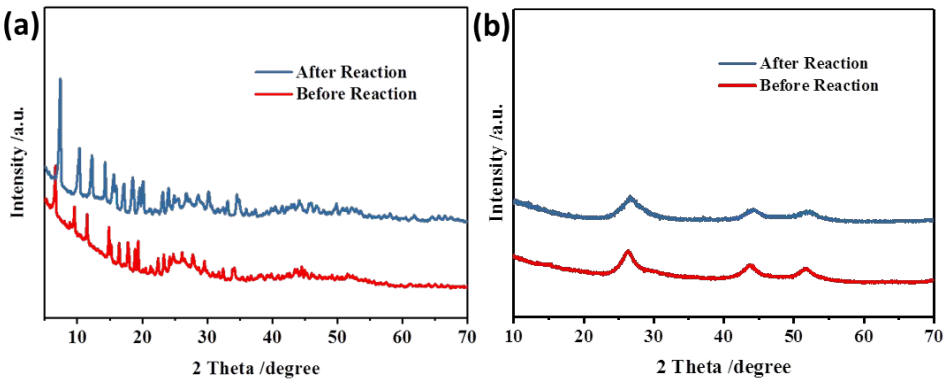

Figure S12. XRD patterns of (a) CdS/Pt4/MIL-125 and (b) CdS before and after five cycling tests.

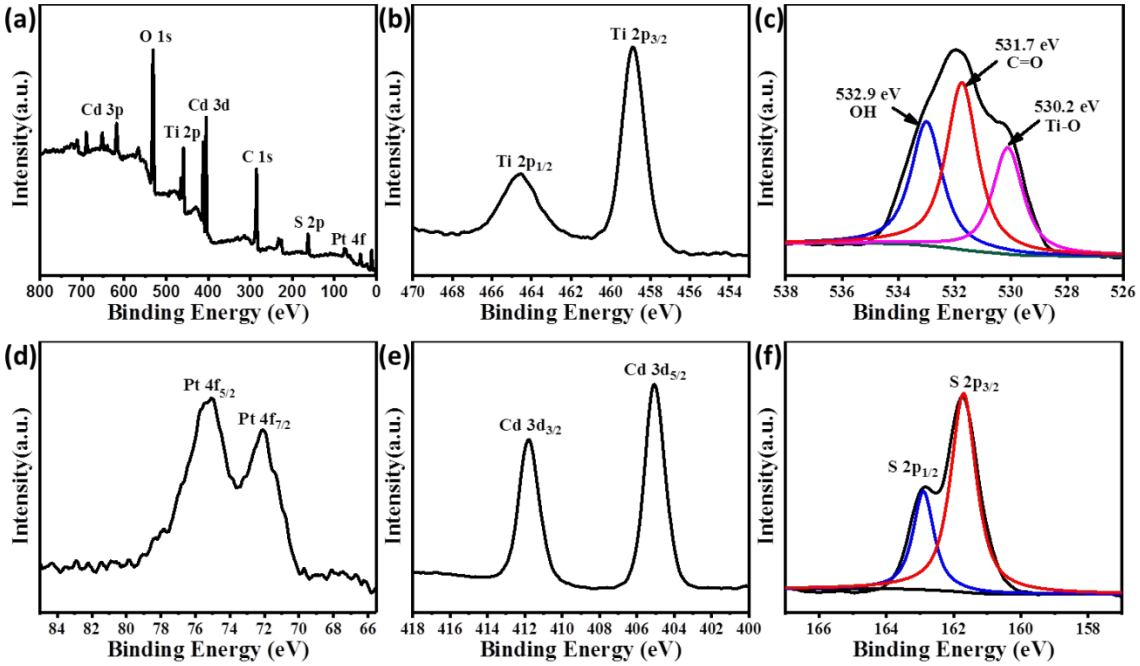

Figure S13. (a) XPS survey scan of the CdS/Pt4/MIL-125 catalyst after five cycling tests and the corresponding high-resolution XPS spectra: (b) Ti 2p; (c) O 1s; (d) Pt 4f; (e) Cd 3d; (f) S 2p.

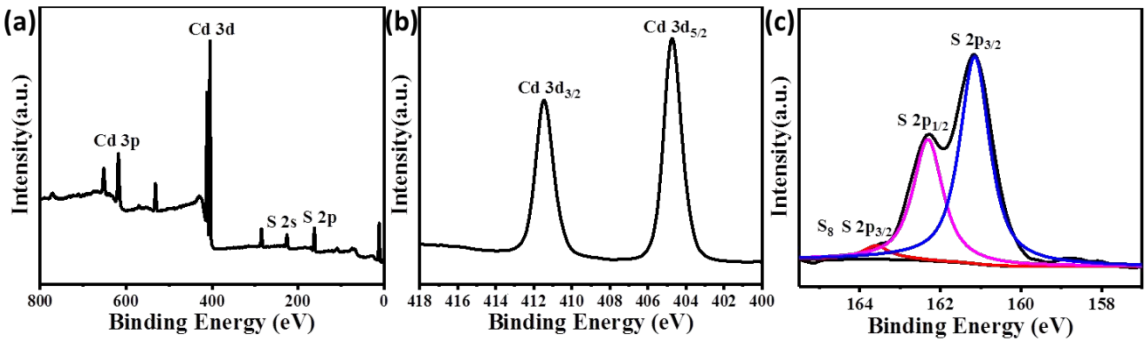

Figure S14. (a) XPS survey scan of the CdS nanoparticles after five cycling tests and the corresponding high-resolution XPS spectra: (b) Cd 3d; (c) S 2p.

REFERENCES

(S1) Zhao, H.; Wu, M.; Liu, J.; Deng, Z.; Li, Y.; Su, B. L. Synergistic promotion of solar-driven H_2 generation by three-dimensionally ordered macroporous structured TiO_2-Au-CdS ternary photocatalyst. *Appl. Catal. B* **2016**, *184*, 182-190. DOI 10.1016/j.apcatb.2015.11.018.

(S2) Peng, R.; Zhao, D.; Baltrusaitis, J.; Wu, C. M.; Koodali, R. T. Visible light driven photocatalytic evolution of hydrogen from water over CdS encapsulated MCM-48 materials. *RSC Adv.* **2012**, *2*, 5754-5767. DOI 10.1039/C2RA20714A.

(S3) Yuan, W.; Zhang, Z.; Cui, X. L.; Liu, H. R.; Tai, C.; Song, Y. R. Fabrication of hollow mesoporous CdS@TiO_2@Au microspheres with high photocatalytic activity for hydrogen evolution from water under visible light. *ACS Sustainable Chem. Eng.* **2018**, *6*(11), 13766-13777. DOI 10.1021/acssuschemeng.8b01787.

(S4) Zhao, H.; Dong, Y. M.; Jiang, P. P.; Wang, G. L.; Miao, H. Y.; Wu, R. X; Kong, L. G.; Zhang, J. J.; Zhang, C. Light-assisted preparation of a ZnO/CdS nanocomposite for enhanced photocatalytic H_2 evolution: an insight into importance of in situ generated ZnS. *ACS Sustainable Chem. Eng.* **2015**, *3*, 969-977. DOI 10.1021/acssuschemeng.5b00102.

(S5) Xu, H. Q.; Yang, S. Z.; Ma, X.; Huang, J. E.; Jiang, H. L. Unveiling charge separation dynamics in CdS/MOF composites for enhanced photocatalysis. *ACS Catal.* **2018**, *8*, 11615-11621. DOI 10.1021/acscatal.8b03233.

(S6) Bibi, R.; Huang, H. L.; Kalulu, M.; Shen, Q. H.; Wei, L. F.; Oderinde, O.; Li, N. X.; Zhou, J. C. Synthesis of amino-functionalized Ti-MOF derived yolk-shell and hollow heterostructures for enhanced photocatalytic hydrogen production under visible light. *ACS Sustainable Chem. Eng.* **2019**, *7*(5), 4868-4877. DOI 10.1021/acssuschemeng.8b05352.